

Original Paper

Experimentally Induced Convulsive Seizures Are Modulated in Part by Zinc Ions through the Pharmacoresistant Ca_v2.3 Calcium Channel

Serdar Alpdogan^a Felix Neumaier^a Jürgen Hescheler^a Walid Albanna^b
Toni Schneider^a

^aInstitute for Neurophysiology, University of Cologne, Köln, Germany, ^bDepartment of Neurosurgery, RWTH Aachen University, Aachen, Germany

Key Words

Epilepsy • Voltage-gated Ca_v2.3 calcium channels • Epilepsy • EEG • Zinc • Kainic acid • Intracerebroventricular injections

Abstract

Background/Aims: Still in 1999 the first hints were published for the pharmacoresistant Ca_v2.3 calcium channel to be involved in the generation of epileptic seizures, as transcripts of alpha1E (Ca_v2.3) and alpha1G (Ca_v3.1) are changed in the brain of genetic absence epilepsy rats from Strasbourg (GAERS). Consecutively, the seizure susceptibility of mice lacking Ca_v2.3 was analyzed in great detail by using 4-aminopyridine, pentylene-tetrazol, N-methyl-D-aspartate and kainic acid to induce experimentally convulsive seizures. Further, γ -hydroxybutyrolactone was used for the induction of non-convulsive absence seizures. For all substances tested, Ca_v2.3-competent mice differed from their knockout counterparts in the sense that for convulsive seizures the deletion of the pharmacoresistant channel was beneficial for the outcome during experimentally induced seizures [1]. The antiepileptic drug lamotrigine reduces seizure activity in Ca_v2.3-competent but increases it in Ca_v2.3-deficient mice. *In vivo*, Ca_v2.3 must be under tight control by endogenous trace metal cations (Zn²⁺ and Cu²⁺). The dyshomeostasis of either of them, especially of Cu²⁺, may alter the regulation of Ca_v2.3 severely and its activity for Ca²⁺ conductance, and thus may change hippocampal and neocortical signaling to hypo- or hyperexcitation. **Methods:** To investigate by telemetric EEG recordings the mechanism of generating hyperexcitation by kainate, mice were tested for their sensitivity of changes in neuronal (intracerebroventricular) concentrations of the trace metal cation Zn²⁺. As the blood-brain barrier limits the distribution of bioavailable Zn²⁺ or Cu²⁺ into the brain, we administered micromolar Zn²⁺ ions intracerebroventricularly in the presence of 1 mM histidine as carrier and compared the effects on behavior and EEG activity in both genotypes. **Results:** Kainate seizures are more severe in Ca_v2.3-competent mice than in KO mice and histidine lessens

seizure severity in competent but not in Ca_v2.3-deficient mice. Surprisingly, Zn²⁺ plus histidine resembles the kainate only control with more seizure severity in Ca_v2.3-competent than in deficient mice. **Conclusion:** Ca_v2.3 represents one important Zn²⁺-sensitive target, which is useful for modulating convulsive seizures.

© 2020 The Author(s). Published by
Cell Physiol Biochem Press GmbH&Co. KG

Introduction

Calcium (Ca²⁺) influx through voltage-gated Ca²⁺ channels (VGCCs) participates in excitation-contraction coupling of muscles [2, 3], in excitation-secretion coupling during peptide hormone and neurotransmitter release [4-6], in excitation-transcription coupling during Ca²⁺-mediated regulation of development [7] and in apoptosis regulation [8]. Thus, the expression and function of VGCCs is under tight cellular control. In mammals, 10 members of VGCCs are known: the L-type (Ca_v1.1, Ca_v1.2, Ca_v1.3 and Ca_v1.4), P / Q - type (Ca_v2.1), the N-type (Ca_v2.2), the R-type (Ca_v2.3), and the T-type channels (Ca_v3.1, Ca_v3.2, and Ca_v3.3) [9-11]. Several ion conducting Ca_vα1-subunits [12, 13] and many native Ca²⁺ currents [14, 15] are antagonized by inorganic cations, which have long been used to block voltage-gated Ca²⁺ channels (for review, see: [16]). Especially the pharmacoresistant voltage-gated Ca²⁺ channel (R-type) containing the Ca_v2.3 α1-subunit as ion conducting pore [17], has been shown to represent the most sensitive molecular target of Cu²⁺ currently known [18]. Low nanomolar concentrations are sufficient to tonically inhibit these channels and to markedly shift voltage-dependent gating towards more depolarized potentials. Structurally, the exceptionally high sensitivity results from two histidine residues in the IS3-IS4 loop (His¹⁷⁹ and His¹⁸³) and a third one located in the IS1-ISE loop (His¹¹¹) of the Ca_v α1-subunit [18, 19]. Thus, the binding site is located outside the cell but the blood brain barrier inhibits easy access of administered divalent cations to the R-type Ca²⁺ channels in the nervous system. Therefore, cannulas were implanted to administer zinc ions and histidine intracerebroventricularly and to test effects of altered trace metal homeostasis after KA-induced epilepsy in mice, which is a well-established method for generating temporal lobe epilepsy causing multiple pathological changes including degeneration of pyramidal neurons in the hippocampus [20-22]. Furthermore, in our previous studies we could also demonstrate Ca_v2.3 KO mice are more resistant to the convulsive effects of KA [23].

Several technical issues have to be considered for the chronic implantation of intracerebroventricular (ICV) guide cannulas and the injection of trace metal containing solutions [24]. (i) Any uncontrolled contamination by trace metals must be prevented and therefore metal free cannulas were used as described in detail recently [25]. (ii) Further, the background level of trace metal contamination in physiological solutions strongly must be reduced. (iii) Different from other biologically relevant divalent cations, such as Ca²⁺ and Mg²⁺, free concentrations of trace metals in the brain are extremely low and strictly regulated by a variety of metalloproteins [26]. In the healthy brain, concentrations of Zn²⁺ and Cu²⁺ are estimated to be around 70-150 μM [23], and most of them (>95%) are protein bound. Local free or loosely bound concentrations of Zn²⁺ and Cu²⁺ can reach 30 μM [27] and 1.7 μM [23], respectively. Thus, during the injection of trace metals into the ventricles, histidine may be used as a chelator instead of metalloproteins, and its application to enable Zn²⁺ injection into the CNS will be described in detail.

Materials and Methods

Injection cannulas and injection conditions

For the *in vivo* research of trace metal cation injections, the Cannula Infusion System (Bilaney Consultants GmbH, Düsseldorf / Germany) consisting of a guide cannula, an internal cannula and a dummy cannula was used. The guide cannula was implanted onto the mouse head and used to guide the internal cannula to a specified depth. A so-called dummy cannula inserts into the guide cannula to protect the brain when there is no infusion or delivery taking place. The internal cannula is used to deliver trace metal cations or control substances in isotonic NaCl solution intracerebroventricularly. The cannula components are made of polyether ether ketone (PEEK, Plastics One Inc., Roanoke, VA, USA), an advanced biomaterial, which is used in medical implants and for optogenetic studies. Further details were reported recently [24].

Telemetry system

Telemetry recordings were performed from conscious mice, after more than 7 days of recovery from the implantation procedures as described in detail [28]. The system used consists of a telemetry implant (PhysioTel® transmitter TA10ETA-F20) for mice of a body weight larger than 20 g with the technical specification as: 3.9 g, 1.9 cc, and bandwidth of frequency transfer of 1-200 Hz (from Data Science International, DSI, Lexington, USA) capable of recording biopotentials such as electroencephalogram (EEG), electrocardiogram (ECG), electromyogram (EMG), physical activity, and temperature. It was used with a nominal sampling rate of 1000 Hz. The temperature operating range lies between 34-41° Celsius with a battery lifetime of 4 months.

The smaller and lighter PhysioTel® ETA-F10 transmitter (frequency range 1-200 Hz), is the recommended replacement for ETA-F20 and represents an optimized version, which can be implanted in mice with a body weight of larger than 17 g to measure biopotentials (ECG, EEG or EMGs), temperature and activity data. In both transmitter variants, the battery can be turned on - off magnetically to save battery life time.

EcoG analysis

Neuroscore 2.1.0 (Datascience International, Lexington, USA) was used to calculate absolute and relative power of frequency bands (Fast Fourier Transform based using a Hamming window) for 2 hours after KA injection (totally and fractioned into 5 min intervals). The frequency spectrum was defined as follows: Delta (0.5-4 Hz), Theta (4-8 Hz), Alpha (8-12 Hz), Sigma (12-16 Hz), Beta (16-24Hz) and Gamma (30-80 Hz). Ripples (80-200 Hz) and Fast Ripples (here only 200-250 Hz), which could not exactly be determined because of the limitation of the bandwidth of the transmitters in use. Original traces were compared with videorecordings to inspect EEG recordings for artefacts. Additionally, an automated seizure detection protocol was written to quantify ictal activity. The protocol recognizes waveforms shorter than 200 ms in length that are between 2.5- and 25-fold the baseline amplitude as spikes. Spikes occurring in intervals between 30 and 1000 ms are recognized as belonging to a spike train which must be at least 300 ms long and contain a minimum of four spikes. No ictal events were detected in the control condition (before KA injection).

Behavioral assesement

As in our previous studies [21, 24] a scoring scale from 0 to 8 was adapted and modified from Morrison et al. [29] for the observation period of 2 hours after injection procedure and divided into 5 min intervals. For each interval, the highest scoring stage was noted and summed to a total score at the end. Normal behavior (stage 0) like grooming, scratching, digging, sniffing, exploring ceased within a few minutes after injection of kainate entering the stage 1 which is described as immobility stage where the animal remains motionless with the tail often appearing straight and stiff and the head is facing straight ahead. Stage 1 is often interrupted by normal behavior or automatisms, head bobbing / nodding representing stage 2. In stage 3 mice exhibit single jerks of the extremities. Rearing, where the mouse is standing straight up on his hind limbs while staring into space with extending and jerking the fore limbs and stargazing are characteristic for stage 4 which is often followed by stage 5 where the mouse is not able to remain on its feet and repetitively fall over. Tonic-clonic seizures evolve in stage 6 with additional uncontrolled jumping behavior (stage 7). Stage 8 characterizes the death of the animal.

Chemicals

Unless noted otherwise, reagents were obtained from Sigma-Aldrich and used without further purification (Sigma-Aldrich / Merck, Schnellendorf, Germany). Substances were injected in sterile isotonic 0.9 % (m/v) sodium chloride solution (KabiPac®, Fresenius Kabi, Bad Homburg, Germany). Zincchloride (ZnCl₂) was purchased from Sigma as a stock solution (0.1 M ZnCl₂, ordering number 03363) and was further diluted in sterile isotonic 0.9 % NaCl to a final concentration of 10 μM for the intracerebroventricular injection. L-histidine (99.5 %) was purchased from Sigma and was used in a concentration of 1 mM. ZnCl₂ (10 μM) and L-histidine (1 mM) were coinjected in a total volume of 3 μl during a 2 min period. Glutamate free kainic acid monohydrate (>99%) was purchased from Milestone Pharmtech (New Brunswick, NJ, USA).

Animals and housing

In total, 55 male Ca_v2.3-competent and 57 Ca_v2.3-deficient mice were used in this study, but 2 WT and 1 KO mice were excluded from further data analysis due to a lost lead connection or categorized as a non-responder. All mice have a mixed genetic background (C57Bl/6 and 129SvJ) and were used at the age of 17.6 ± 0.2 wks (controls) and 17.5 ± 0.2 wks (Ca_v2.3-/-). They housed at a constant temperature (20°C-22°C) in polycarbonate cages (26.5 cm x 20.5 cm x 14.5 cm) under standardized housing conditions with light on from 7 a.m. to 7 p.m. (light intensity at the surface of the animal cages was between 5 and 10 lux), relative humidity of 40-48 % and ad libitum access to food and water. After the implantation procedure animals were individually housed in separate cages and observed frequently to maintain full recovery after surgery. During the recovery period, body weight was measured daily. The animal experimentation described in the text was approved by the institutional committee on animal care and conducted in accordance with accepted standards of human animal care. All animal experiments were in line with the European Communities Council Directive 2010/63/EU for the care and use of laboratory animals, and as described in the UFAW handbook on the care and management of laboratory animals.

Transmitter implantation and placement of the guidance cannulas

Anesthesia and pain treatment. Mice were anesthetized with 100 mg / kg body weight (BW) ketamine hydrochloride (KETASET, Zoetis, New Jersey, USA) and 10 mg / kg BW xylazine hydrochloride (Rompun® 2% Bayer Vital, Leverkusen, Germany) for transmitter implantation and fixation of guidance cannula. During the whole surgical procedure mice were placed on a thermoregulated operation table to prevent hypothermia. Carprofen (5 mg / kg) (Rimadyl® Pfizer, New York, USA) was administered subcutaneously for pain management.

Surgery procedure for transmitter implantation, and placement of electrodes and cannulas. The time needed for the combined surgery procedure is between 30 to 45 min. The surgery for the implantations were performed on a warming plate (295 mm x 245 mm x 70 mm, MEDAX GmbH & Co.KG, Neumünster, Germany) to keep the body temperature at 37-38°C (98.6-100.4 °F). To avoid corneal desiccation, eyes were covered with dexpanthenol (Bepanthen®, Hoffmann-La Roche AG) during the implantation period and early recovery. A standard stereotaxic frame, which had been modified to fit the mouse skull anatomy, was used as described previously [28] to locate the targeted area for intracerebroventricular injection at position -0.34 mm from bregma and lateral -1 mm in the os parietale and for correct electrode placement at coordinates caudal -1 mm from bregma and lateral 3 mm (somatosensory cortex) for the different electrode lead and for the indifferent electrode at the coordinate caudal -6.3 mm from bregma and lateral 1 mm (close to the sutura sagittalis). Teeth holder and nose clamp as well as the ear bars had been adapted. After the recovery from the surgery procedure (at least 7 days), the mouse cage was placed on individual receiver plates for the recording of EEGs. The detailed procedure for the transmitter implantation and the epidural fixation of electrodes and cannula will be described in the Supplemental Material file (for all supplemental material see www.cellphysiolbiochem.com).

Injections. All animals were allowed to recover from the implantation procedure for 7 days before intracerebroventricular injections of histidine or trace metal cations and saline or kainic acid occurred. Baseline EEGs of the mice were recorded twenty-four hours before the injections were started.

ICV injections of trace metal cations were performed under isoflurane gas anesthesia via the implanted guide cannula leading to one of the lateral ventricles while kainic acid or saline was injected intraperitoneally.

Injection procedure in detail for trace metal cations:

a. After recording spontaneous EEGs as a baseline control, the mouse is anesthetized with isoflurane while applying ZnCl₂ (10 μM ZnCl₂ + 1 mM histidine in saline) or histidine only in saline via the guide cannula. Injection speed was 0.15 μl per min and in total 0.3 μl.

b. Injection of kainic acid (15 mg/kg body weight in saline) or saline intraperitoneally 0.1 ml/10 g body weight.

c. Mouse gets placed back into its cage and the receiver plate and recordings and behavioral observations are started.

Verification of the cannula position and access to the brain ventricle:

Postmortem Indian ink was injected through the guide cannula with an injection cannula. The brain was fixed in 4 % paraformaldehyde and was extirpated from the skull. The brain was cut in half in the sagittal plane and the spread ink was found in all four ventricles, verifying that the guide cannula was properly placed over the lateral ventricle.

Data analysis and statistics

Distribution of seizure scores, Neuroscore data and relative spectral power values were assessed using Shapiro-Wilk test of normality and were found to be mostly non-normally distributed. Therefore, the nonparametrical Mann-Whitney test was used to determine significance of seizure scores and Neuroscore data. Data of relative spectral power showed up to be mostly normally distributed and therefore were tested with student's t-test for significance. For non-normally distributed values again the Mann-Whitney test was used and marked with stars in the Supplementary Tables. All values are expressed as mean ± SEM based on n, the number of independent experiments. P-values of 0.05 and below were considered significant.

Results

Postoperative recovery and body weight development

Fifty-three controls and fifty-six Ca_v2.3-deficient male mice with no statistical difference of age (17.6 to 17.5 wks, p = 0.69) were investigated. The body weight of treated mice was monitored daily and at this age the body weight of Ca_v2.3-deficient mice (28.6 ± 0.4 g) was slightly and significantly lower than in control animals (31.3 ± 0.4 g) (see Supplementary Fig. S1A), which may be caused by deficits in peptide hormone release of glucagon [30, 31], insulin release [32-34] and somatostatin [35].

All mice were checked for infection, pain or discomfort and treated when necessary with analgetics (5 mg/kg carprofen, twice a day). Pain and discomfort were recognized in individuals by analyzing behavioral changes such as a lowered locomotion, lowered grooming behavior a lowered food intake and also by evaluation of the physical appearance of the mouse for example if the area of the eyes is narrowed or the cheek and nose is bulged. Eating normal pellets and normal nesting behavior as well as fur care and explorative behavior was observed at the latest after 2 to 3 days after the surgery. It was observed that Ca_v2.3-competent mice lost more weight 1 day after operation procedure (from 100% of initial bodyweight to 98.4 %, p = 0.007) than Ca_v2.3-deficient mice (100 % of initial body weight to 98, 8 %) suggesting a faster recovery. During recovery time the body weight was followed up for both genotypes separately and used as an additional measure for the progress during recreation (see Supplementary Fig. S1B).

ECoG recordings before and after KA injection (15 mg/kg)

Control electrocorticograms (ECoGs) for both genotypes were recorded for 24 hours before KA was injected (see Supplementary Fig. S2). During this time spontaneous EEG traces were collected lacking any extended spike trains, which however arose as soon as KA (15 mg/kg bw) was injected intraperitoneally (see Supplementary Fig. S3 and S4). Six different groups of mice were investigated (for details see Table 1). Subgroup 1 and 2 (in group A) did not have implanted epidural cannulas and the spontaneous EEGs as well as the behavior did not differ before the injection of KA [24]. Further, mice with implanted cannulas from both

genotypes did not show convulsive seizures, abnormal ECoG traces or any indication of a status epilepticus, neither after i.c.v. injection of L-histidine (1 mM) (Supplementary Fig. S2A and S2C), nor after i.c.v. injection of histidine plus $ZnCl_2$ (10 μ M) (Supplementary Fig. S2B and S2D).

However, after (additional) i.p. injection of kainate (KA) epileptic discharges were recorded from both genotypes (Supplementary Fig. S3 and S4). As in earlier studies, the i.p. injection of KA induced ictal activity starting with single spiking and led to an increased frequency of spikes and spike-and-waves.

In subgroup number 2, 4 and 6 (mice injected with KA, Table 1) convulsive seizures developed differently in $Ca_v2.3$ -competent and $Ca_v2.3$ -deficient mice (Fig. 1). Time to reach the higher score stages 6 (tonic-clonic seizures) and 7 (tonic-clonic seizure with jumping) (Fig. 1A, 1B) did not significantly differ between both genotypes and more $Ca_v2.3$ (+/+) mice reached score 6 and 7 (6 out of 7 mice) but only 5 out of 9 for $Ca_v2.3$ (-/-) mice. After histidine co-injection with kainate, only one out of 11 $Ca_v2.3$ -competent mice, and only one out of 10 $Ca_v2.3$ -deficient mice died (Fig. 1C). The co-injection of Zn^{2+} plus histidine with kainate raised the number of dying mice to 6, only for $Ca_v2.3$ -competent mice in contrast to $Ca_v2.3$ (-/-) mice, where all of them survived, suggesting that the antagonism by low Zn^{2+} of $Ca_v2.3$ (in the presence of histidine) is involved in the seizure-induced dying of mice increasing the risk of status epilepticus only in $Ca_v2.3$ -competent mice (Fig. 1C).

The data from the behavioral investigation were analyzed to compare the KA effect on both genotypes under the three different KA-conditions by quantifying the maximal behavioral scores ("max") reached during the two hour observation period (Fig. 2A and 2B).

Injecting kainate in the presence of histidine reduced significantly the maximum score numbers compared to kainate without any i.c.v. injection only in $Ca_v2.3$ -competent mice (Fig. 2A). No significant differences were found for $Ca_v2.3$ -deficient mice (Fig. 2B).

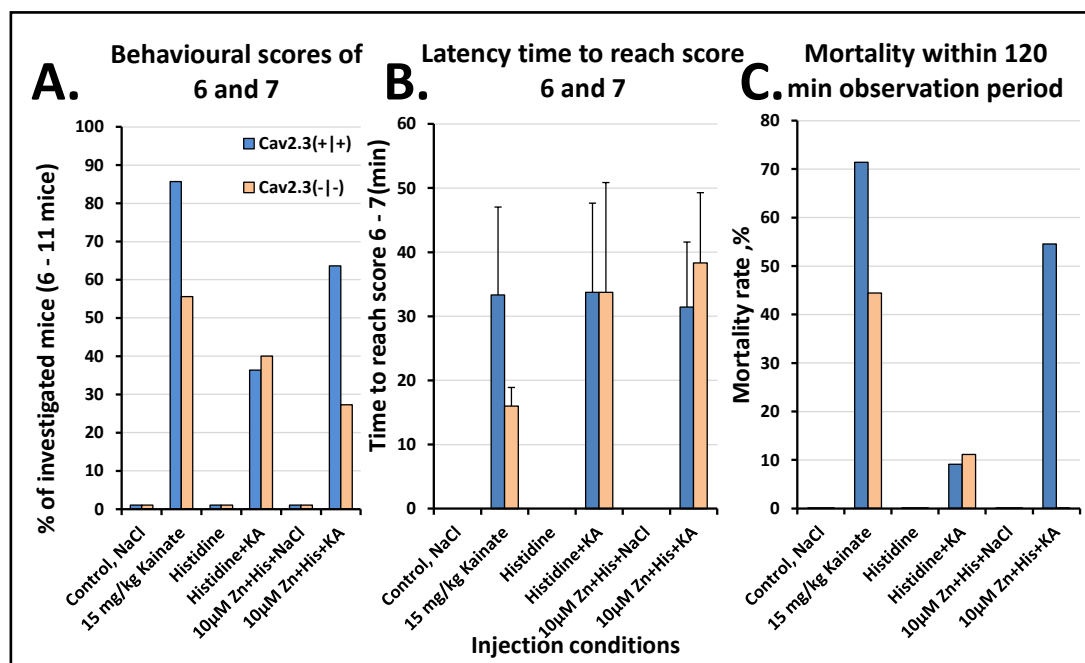


Fig. 1. Effect of i.p. kainate (15 mg/kg) on behavior and survival rate. The mice ($n = 6$ to 11) in control groups without kainate never reached the scores of 6 or 7 (panel A.) during the behavioral analysis (evaluation using an adapted version of Morrison's Seizure Rating Scale (Morrison et al., 1996, as described in Dibué-Adjei et al., 2017). Panel B shows changes in latency time depending on different KA injections. None of the mice died during the 2 hour observation period. Only after kainate injection mice died after reaching stage number 8 (panel C.).

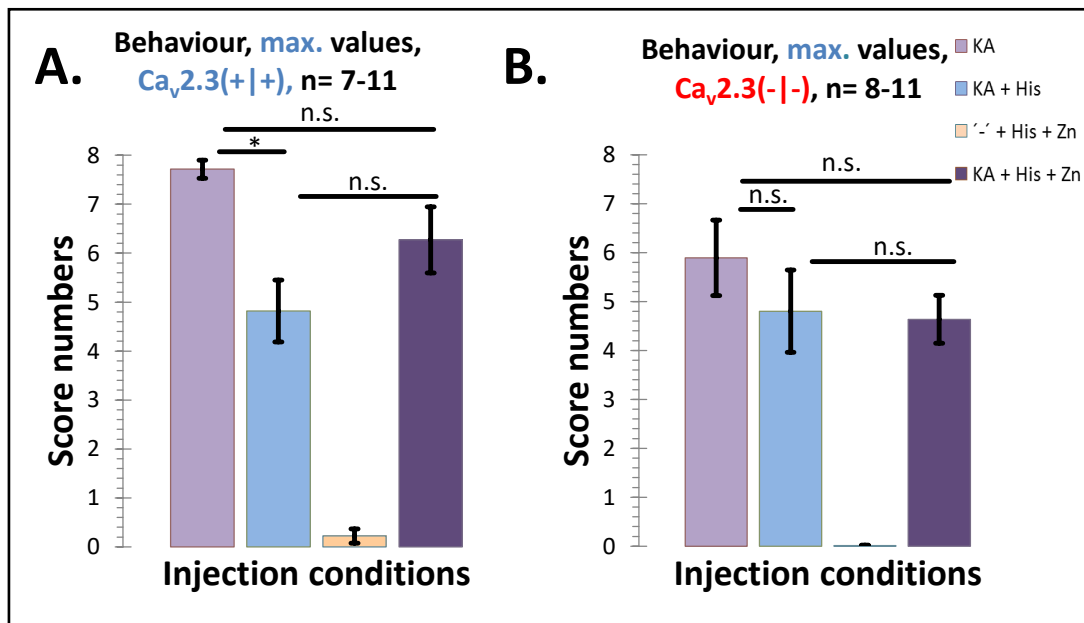


Fig. 2. Behavioral seizure analysis. Effect of i.p. injection of kainate (15 mg/kg) on behavioral scores. The initial 2 hours after the application of KA or saline were evaluated using an adapted version of Morrison's Seizure Rating scale [29]. Only when kainate was injected, normal explorative behavior ceased within ten minutes and higher seizure stages were developed during the observation period. Under histidine with no kainate, or under Zn-histidine with no kainate, most of the time normal behavior (stage 0) was observed. Only in six out of 50 mice (both genotypes) stage 1 was reached (immobility, exhibiting a rigid posture and staring into space). A. Higher seizure scores evaluated as maximal scores (score 6 and/or 7) are plotted for Ca_v2.3-competent mice (Ca_v2.3+/+). For comparison reasons, maximal scores for the injection of histidine (1 mM) plus ZnCl₂ (nominally 10 μM) without KA-injection was shown, which is close to zero. B. Higher seizure scores evaluated as maximal scores (score 6 and/or 7) are plotted for Ca_v2.3-deficient mice (Ca_v2.3-/-). For comparison reasons, maximal scores for the injection of histidine (1 mM) plus ZnCl₂ (nominally 10 μM) without KA-injection was shown, which is close to zero.

Spike patterns in ECoGs before and after KA injection

EEG traces were further analyzed by NEUROSCORE 2.1.0 (Datascience International) for the total number of spike trains (Fig. 3A), the total and the average spike train duration (Fig. 3B and 3C), the longest and the shortest spike train duration (Fig. 3D and 3E) and the average number of spikes per train (Fig. 3F). The scatter between the three groups under KA is still large, but shows important differences when comparing between both genotypes and under KA. In Ca_v2.3-competent mice, the total number of spike trains increases significantly after KA without histidine (from 0.8 ± 0.7 to 184 ± 53 $p = 0.001$) or in the presence of Zn-histidine (from 13 ± 9 to 147 ± 42 $p = 0.001$), but not significantly with histidine only (3 ± 1 to 94 ± 41 $p = 0.052$) (for Ca_v2.3-competent mice, see also [24]). Comparing the KA-mediated increases between Ca_v2.3-competent and -deficient mice, reveals significant difference in group C. For Ca_v2.3-deficient mice, the total number of spike trains was significantly changed after KA with Zn-histidine (from 4 ± 2 to 37 ± 15 $p = 0.01$) but significantly less ($p = 0.02$) than for Ca_v2.3-competent mice (from 13 ± 9 to 147 ± 42 $p = 0.00$). Similar genotype specific differences after KA were found for the total and the longest spike train duration (Fig. 3B and 3D, each in group C), for average spike train duration (Fig. 3C, group A), and for the average number of spikes per train (Fig. 3F, group A) (for further details, see Supplementary Tables S1 to S4).

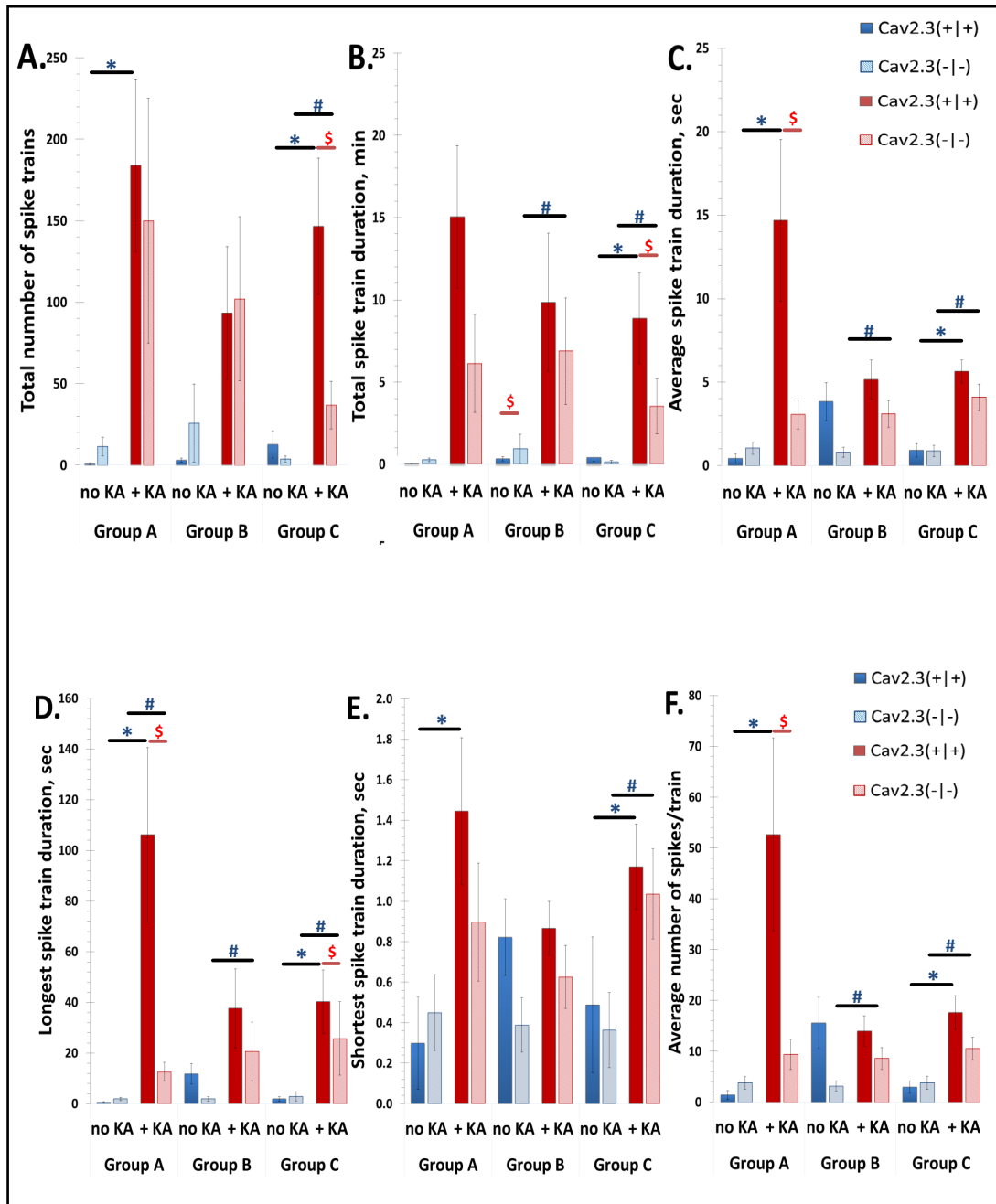


Fig. 3. A-F Mean values of EEG spike patterns (Neuroscore). EEG recordings were evaluated with an automated protocol, which was written to identify seizure activity. A spike was recognized when ictal activity was shorter than 200 ms and exceed 2.5- to 25- fold the baseline amplitude with a minimum value of 125 μ V. Spike trains were defined when at least a minimum of 4 spikes was included which occur in intervals between 30 and 1000 ms. This spike train should have a minimum duration of 300 ms. For further details, see text. Error bars represent SEM values (Mann-Whitney-U-Test ; $p < 0.05$ was marked as significant with red dollar sign for differences between both genotypes and with blue stars for differences within a genotype).

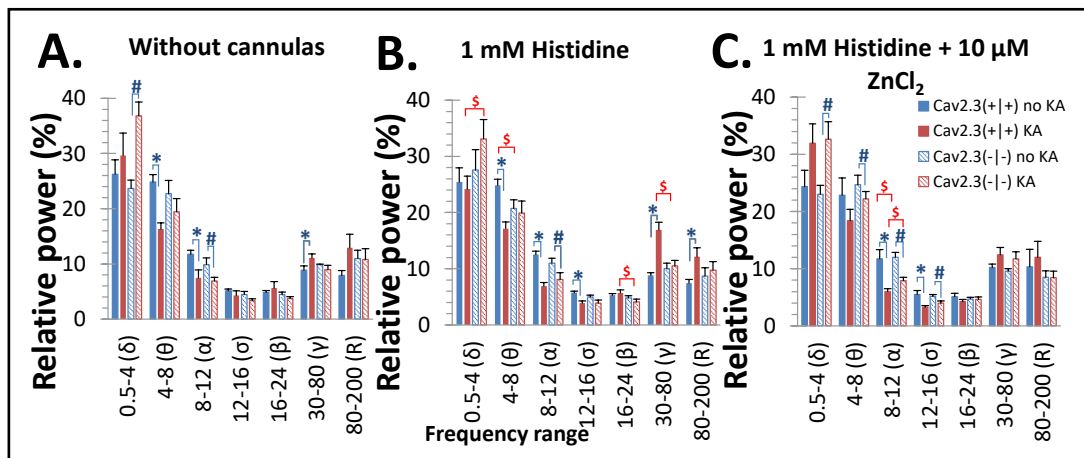


Fig. 4. Power-spectrum density (PSD) analysis of ictal episodes for the various frequency ranges. Relative power was used in the evaluation and statistical testing due to better inter-individual comparability. Lines and asterisks (*) and diamonds (#) in blue color highlight the differences between mice without and with KA i.p. injection (15 mg/kg bw). Statistical differences are significant for $p < 0.05$. Lines in red color highlight the differences between both genotypes, and statistical differences are significant for $p < 0.05$ (\$).

Power spectrum density analyses

To receive a deeper insight into the differences between both genotypes during the KA-induced development of convulsive seizures, a power-spectrum density (PSD) analysis was performed for all groups (Fig. 4). During the previous Neuroscore data analysis (Fig. 3A-F) the parameters did not show any significant differences between both genotypes in the subgroups 3/4 (group B in Fig. 3A-F). Contrary to this the highest number of parameter now differed in group B during the PSD analysis (the number of \$-signs in Fig. 4B). The comparisons will be grouped and are color-coded for (i) differences between both genotypes and (ii) the differences within each genotype for the conditions without and with KA-injection. Significant differences according to (i) are labeled with a red dollar sign, and significant differences according to (ii) are labeled with stars in blue for WT and blue diamond for KO mice (Fig. 4).

In group A (no cannulas, Fig. 4A) changes occur in both genotypes. KO mice show a significant increase for the delta power under KA and a decrease in alpha power, but WT mice show instead a significant increase in gamma power as well as a reduction in theta- and alpha power (Fig. 4A; for details see Supplementary Table S5).

As mentioned, in group B (histidine groups, Fig. 4B) the highest number of power-parameters varied between the different conditions. Similar as for the WT in group A, theta and gamma power changed, even with higher significance now (Fig. 4B). Further, the power in the alpha, sigma and ripple frequency range varied significantly for the WT mice. The only frequency range which was significantly affected for KO is the alpha range. In groups 3/4 KA reduced in WT mice the power in the theta, alpha and sigma range and raised the power in gamma and the range for ripples. Genotypic differences are observed in 4 frequency ranges (delta-, theta-, beta- and gamma frequency) in this group. Comparing WT vs KO mice KA reduces theta beta and gamma power in KO mice while delta power is raised up in KO mice (Fig. 4B; for details see Supplementary Table S6).

In the last group C (histidine plus 10 μ M ZnCl₂, Fig. 4C), significant differences of power centered in the alpha- and sigma set of frequencies for both genotypes and additionally for KO mice in the delta and theta frequency range. KA related differences are observed in both genotypes. The power for theta, alpha and sigma was reduced significantly and in the delta range the frequency power was raised for KO mice. Additionally, genotypic different effects are observed for the alpha frequency (Fig. 4C; for details see Supplementary Table S7).

Discussion

Recently, the *in vivo* analysis of the physiological role of Ca_v2.3 during epilepsy gained more attention, because in humans about 30 *de novo* mutations were found in Ca_v2.3 causing epileptic encephalopathies with fatal outcomes [36]. Therefore, any drug or pathway, which may modulate pathophysiologically changed activities of Ca_v2.3, may help to develop novel therapeutic approaches to cure the mentioned fatal encephalopathies, as it still was shown for 5 patients by the application of topiramate [36, 37].

The present report gives additional hints how therapeutical approaches must be planned. The main results of the present study reveal that variations of divalent metal cation concentrations in the murine CNS either by chelation by histidine (1 mM) or by adding ZnCl₂ (10 μM) affect the sensitivity towards kainate induced epileptic seizures. An optimized Zn²⁺ concentration may be protective towards convulsive seizures.

Effects of histidine and Zn²⁺ on neuronal excitation in Ca_v2.3-competent and -deficient mice

Structure and properties of histidine and its complexes with metal cations. The essential amino acid histidine is needed for the production of histamine but also to regulate and utilize essential trace minerals such as copper, zinc, iron, manganese, and molybdenum [38, 39]. It is well known to act as a sensitive chelator for these divalent metal cations [40]. The strongest affinity to L-histidine was reported to be exhibited by the Cu²⁺ cation. By using computational chemistry, not only divalent but also monovalent cations were found to form complexes with L-histidine as charge-solvated and salt bridge His M (M = Li⁺, Na⁺, K⁺, Mg²⁺, Ca²⁺, Ni²⁺, Cu²⁺) (for details, see: [40]).

(Sub-) micromolar Zn²⁺ concentrations in the CNS and its role during experimentally induced seizures. Low concentrations of Zn²⁺ modulate the activity of a multitude of voltage- or ligand-gated ion channels (see Table 1 in: [41]). Zn²⁺ can be actively released in glutamatergic synapses during neurotransmission and its release correlates with neuronal activity [42]. Excessive synchronized excitation as seen in epilepsy may generate a zinc overload in the extracellular space. Kainic acid-induced recurrent mossy fiber excitation of dentate gyrus inhibitory interneurons may cause a hyper-inhibition in chronically epileptic mice, similar as seen in epileptic rats [43]. Similar changes of the recurrent inhibition by inhibitory neurotransmitters were observed in the vertebrate retina [44, 45].

Table 1. Injection conditions and number of Ca_v2.3-competent and Ca_v2.3-deficient mice in each group: Kainate (KA) was injected intraperitoneally (15 mg/kg). Histidine (His, 1 mM) was injected intracerebroventricularly, without or in combination with ZnCl₂ (nominally 10 μM)

Genotype, subgroup and injected solutions	Group A		Group B		Group C	
	1. Controls	2. KA	3. Histidine (His)	4. His + KA	5. ZnCl ₂ + His	6. ZnCl ₂ + His + KA
Cannula implantation	-	-	+	+	+	+
Histidine, 1 mM	-	-	+	+	+	+
ZnCl ₂ , 10 μM	-	-	-	-	+	+
Kainate, 15 mg/kg	-	+	-	+	-	+
Isotonic NaCl, ip	+	-	+	-	+	-
Ca _v 2.3(+ +)	6	7	9	11	9	11
Ca _v 2.3(- -)	6	9	9	10	11	11

Changes of spike patterns in ECoGs before and after KA injection (15 mg/kg)

Similar as in previous reports [28], the implantation of the radiofrequency transmitters in a subcutaneous pouch at the flank, close to the ventral abdominal regions and fixed at the skin, yielded sufficient signal strength for a high signal to noise ratio. The electrocorticograms recorded 24 h before or without KA treatment did not show any signs of unphysiological electrical brain activity.

In both genotypes the consecutive KA injection leads to spiking patterns typically seen during epileptic events (Supplementary Fig. S3 and S4). Visual inspection of the spiking patterns reveals that they may be less pronounced in WT mice which have been treated with L-histidine and KA (Supplementary Fig. S3B), which was confirmed by the loss of statistical differences between parameters of both genotypes (Fig. 3A-F). While the average and longest spike train duration as well as average number of spikes per train between control and Ca_v2.3-deficient mice differed significantly with no cannulas (Fig. 3C, D, F) and three parameters differed significantly under ZnCl₂ plus histidine (Fig. 3A, B, D), these parameters dropped down in control mice when histidine was injected only (Fig. 3A, B, D). Additionally, histidine injection alone seems to influence the total spike train duration in WT vs KO (Fig. 3B). These results strongly confirm the beneficial effects for the Ca_v2.3-competent mice and the administration of ZnCl₂ (10 μM) raises Neuroscore parameters indicative for more severe and longer lasting convulsive seizures under KA.

Power spectrum density analyses

For the power spectrum analyses differences of selected frequencies occur between genotypes more often under histidine compared to both other conditions (see red dollar sign in Fig. 4). In addition, more significant differences were also found under histidine when comparing frequency power without or with KA injection (see blue stars in Fig. 4).

Under histidine 5 of 6 significant differences of relative power (theta-, alpha, sigma, gamma-waves and ripples) are observed for the Ca_v2.3-competent but not for the -deficient mice with one exception (alpha power) (Fig. 4B) indicating that the expression of Ca_v2.3 represents a prerequisite for the beneficial effect of histidine injection. Presumably, histidine chelates divalent metal cations in the brain, which, however, may only be partially reversed by co-injection of 10 μM ZnCl₂ with histidine (Fig. 4C). Only the power of the θ-waves, γ-waves and the ripples get reversed but not for α- and θ-waves. These two waves, however, now get significantly different (before / after KA) also for the Ca_v2.3-deficient mice, which may be caused by Zn²⁺ interaction with another target, possibly with the structurally related Ca_v3.2 / T-type Ca²⁺ channel, which also has a high affinity for divalent metal cations [46].

In the following part the possible involvement of the higher frequency oscillations (γ-waves and ripples) in Ca_v2.3-mediated neuronal regulation of excitation will be discussed more in detail focusing on the important question, why does histidine reduce the seizure intensity in Ca_v2.3-competent mice down to levels observed in Ca_v2.3-deficient mice?

For the γ frequency oscillations in the brain, including the hippocampus, it is well known that they may have a role as a reference signal in temporal encoding and they may contribute to memory formation and retrieval [47-51]. In the past, the underlying circuits have been investigated in greater detail. The γ oscillations are generated by a specific class of inhibitory neurons with a robust interconnectivity through fast GABA synapses [52]. Within these neurons fast-spiking parvalbumin (PV)-positive basket cells underlie also the development of gamma oscillations in epilepsy [53]. Using optogenetic activation of hippocampal PV-positive neurons *in vivo*, decreases the duration of spontaneous seizures in a mouse model of temporal lobe epilepsy [54], suggest that the stimulation of PV-positive interneurons may indeed be an appropriate therapeutic avenue in epilepsy.

Pharmacoresistant R-type Ca²⁺ channels have been recorded in inhibitory neurons from several brain regions. The GABAergic tone in the thalamus, which is controlled by inhibitory neurons of the reticular thalamic nucleus, is modulated by presynaptic R-type Ca²⁺ channels [55]. Another example relates to the retinal signal transduction, where Ca_v2.3/R-type channels were shown to be involved into reciprocal inhibition [45, 56].

The present report reveals for injected histidine a beneficial effect for the Ca_v2.3 competent mice during KA induced epilepsy. But the individual frequency bands change in opposite directions as one would expect it, based on the reported literature. During increasing intensity of epileptic seizures, the gamma oscillations are normally increasing [57], which is also observed for the Ca_v2.3 competent mice under histidine, but with concomitant lower seizure intensity as in the mouse groups with no histidine injection.

Conclusion

So far, Ca_v2.3 expressing cells include inhibitory neurons triggering the release of GABA. The specific function of individual interneuron subtypes in the hippocampus but also in the neocortical layers is still not fully understood. The present investigation of experimentally induced epilepsy reveals that i.c.v. histidine injection causes a beneficial effect via the pharmacoresistant Ca_v2.3 Ca²⁺ channel, which is known to have a diverse functional repertoire possibly conditioned by different splice variants in different types of neurons [58] and therefore also disturbs the neuronal homeostasis of bioavailable trace metal cations. The worsening of KA-induced epilepsy by concomitant Zn²⁺ injection with histidine is not only mediated by Ca_v2.3 but also by other high affinity Zn²⁺ receptors as for example via Ca_v3.2, which should be analyzed in the future.

Acknowledgements

We would like to especially thank Mrs. Renate Clemens for her dedication and hard work in this project.

Funding

This study was funded by a DFG /German Research Foundation Grant (Schn 387/21-1 and 21-2).

Disclosure Statement

Part of this study was presented at Annual Meeting of the German and Austrian Society for Epileptology and the Swiss Epilepsy-Liga in Wien, May 3rd – 6th, 2017.

None of the authors has anything other to disclose. We confirm that we have read the Journal's position on issues involved in ethical publication and affirm that this report is consistent with those guidelines.

References

- 1 Weiergräber M; Stephani U, Köhling R: Voltage-gated calcium channels in the etiopathogenesis and treatment of absence epilepsy. *Brain Res Rev* 2010;62:245–271.
- 2 Wagner S, Maier LS, Bers DM: Role of sodium and calcium dysregulation in tachyarrhythmias in sudden cardiac death. *Circ Res* 2015;116:1956-1970.
- 3 Hernandez-Ochoa EO, Schneider MF: Voltage sensing mechanism in skeletal muscle excitation-contraction coupling: coming of age or midlife crisis? *Skelet Muscle* 2018;8:22.
- 4 Almers W, Tse FW: Transmitter release from synapses: Does a preassembled fusion pore initiate exocytosis. *Neuron* 1990;4:813-818.
- 5 Tse A, Lee AK, Tse FW: Ca²⁺ signaling and exocytosis in pituitary corticotropes. *Cell Calcium* 2012;51:253-259.

- 6 Pangrsic T, Singer JH, Koschak A: Voltage-Gated Calcium Channels: Key Players in Sensory Coding in the Retina and the Inner Ear. *Physiol Rev* 2018;98:2063-2096.
- 7 Ma H, Groth RD, Wheeler DG, Barrett CF, Tsien RW: Excitation-transcription coupling in sympathetic neurons and the molecular mechanism of its initiation. *Neurosci Res* 2011;70:2-8.
- 8 Clapham DE: Calcium signaling. *Cell* 2007;131:1047-1058.
- 9 Zamponi GW, Striessnig J, Koschak A, Dolphin AC: The Physiology, Pathology, and Pharmacology of Voltage-Gated Calcium Channels and Their Future Therapeutic Potential. *Pharmacol Rev* 2015;67:821-870.
- 10 Nanou E, Catterall WA: Calcium Channels, Synaptic Plasticity, and Neuropsychiatric Disease. *Neuron* 2018;98:466-481.
- 11 Catterall WA, Wisedchaisri G, Zheng N: The chemical basis for electrical signaling. *Nat Chem Biol* 2017;13:455-463.
- 12 Lee JH, Gomora JC, Cribbs LL, Perez-Reyes E: Nickel block of three cloned T-type calcium channels: Low concentrations selectively block α 1H. *Biophys J* 1999;77:3034-3042.
- 13 Kang HW, Park JY, Jeong SW, Kim JA, Moon HJ, Perez-Reyes E, Lee JH: A molecular determinant of nickel inhibition in Cav3.2 T-type calcium channels. *J Biol Chem* 2006;281:4823-4830.
- 14 Kiss T, Osipenko O: Metal ion-induced permeability changes in cell membranes: a minireview. *Cell Mol Neurobiol* 1994;14:781-789.
- 15 Büsselberg D, Platt B, Michael D, Carpenter DO, Haas HL: Mammalian voltage-activated calcium channel currents are XX blocked by Pb²⁺, Zn²⁺, and Al³⁺. *J Neurophysiol* 1994;71:1491-1497.
- 16 Neumaier F, Dibué-Adjei M, Hescheler J, Schneider T: Voltage-gated calcium channels: Determinants of channel function and modulation by inorganic cations. *Prog Neurobiol* 2015;129:1-36.
- 17 Perez-Reyes E, Schneider T: Calcium channels: Structure, function, and classification. *Drug Dev Res* 1994;33:295-318.
- 18 Shcheglovitov A, Vitko I, Lazarenko RM, Orestes P, Todorovic SM, Perez-Reyes E: Molecular and biophysical basis of glutamate and trace metal modulation of voltage-gated Ca(v)2.3 calcium channels. *J Gen Physiol* 2012;139:219-234.
- 19 Kang HW, Moon HJ, Joo SH, Lee JH: Histidine residues in the IS3-IS4 loop are critical for nickel-sensitive inhibition of the Cav2.3 calcium channel. *FEBS Lett* 2007;581:5774-5780.
- 20 Tremblay E, Ben Ari Y: Usefulness of parenteral kainic acid as a model of temporal lobe epilepsy. *Rev Electroencephalogr Neurophysiol Clin* 1984;14:241-246.
- 21 Dibue-Adjei M, Kamp MA, Alpdogan S, Tevoufouet EE, Neiss WF, Hescheler J, Schneider T: Cav2.3 (R-Type) Calcium Channels are Critical for Mediating Anticonvulsive and Neuroprotective Properties of Lamotrigine In Vivo. *Cell Physiol Biochem* 2017;44:935-947.
- 22 Upadhy D, Kodali M, Gitai D, Castro OW, Zanirati G, Upadhy R, Attaluri S, Mitra E, Shuai B, Hattiangady B, Shetty AK: A Model of Chronic Temporal Lobe Epilepsy Presenting Constantly Rhythmic and Robust Spontaneous Seizures, Co-morbidities and Hippocampal Neuropathology. *Aging Dis* 2019;10:915-936.
- 23 Mathie A, Sutton GL, Clarke CE, Veale EL: Zinc and copper: pharmacological probes and endogenous modulators of neuronal excitability. *Pharmacol Ther* 2006;111:567-583.
- 24 Alpdogan S, Neumaier F, Dibue-Adjei M, Hescheler J, Schneider T (2019) Intracerebroventricular administration of histidine reduces kainic acid-induced convulsive seizures in mice. *Exp Brain Res* 2019;237:481-2493.
- 25 Neumaier F, Alpdogan S, Hescheler J, Schneider T: A practical guide to the preparation and use of metal ion-buffered systems for physiological research. *Acta Physiol (Oxf)* 2018; DOI:10.1111/apha.12988.
- 26 Valko M, Morris H, Cronin MT: Metals, toxicity and oxidative stress. *Curr Med Chem* 2005;12:1161-1208.
- 27 Frederickson CJ, Koh JY, Bush AI: The neurobiology of zinc in health and disease. *Nat Rev Neurosci* 2005;6:449-462.
- 28 Weiergräber M, Henry M, Hescheler J, Smyth N, Schneider T: Electrographic and deep intracerebral EEG recording in mice using a telemetry system. *Brain Res Brain Res Protoc* 2005;14:154-164.
- 29 Morrison RS, Wenzel HJ, Kinoshita Y, Robbins CA, Donehower LA, Schwartzkroin PA: Loss of the p53 tumor suppressor gene protects neurons from kainate-induced cell death. *J Neurosci* 1996;16:1337-1345.
- 30 Pereverzev A, Salehi A, Mikhna M, Renstrom E, Hescheler J, Weiergraber M, Smyth N, Schneider T: The ablation of the Ca(v)2.3/E-type voltage-gated Ca²⁺ channel causes a mild phenotype despite an altered glucose induced glucagon response in isolated islets of Langerhans. *Eur J Pharmacol* 2005;511:65-72.

- 31 Drobinskaya I, Neumaier F, Pereverzev A, Hescheler J, Schneider T: Diethylthiocarbamate-mediated zinc ion chelation reveals role of Cav2.3 channels in glucagon secretion. *Biochim Biophys Acta Mol Cell Res* 2015;1854:953-964.
- 32 Pereverzev A, Vajna R, Pfitzer G, Hescheler J, Klöckner U, Schneider T: Reduction of insulin secretion in the insulinoma cell line INS-1 by overexpression of a calcium channel antisense-alpha1E cassette. *Eur J Endocrinol* 2002;146:881-889.
- 33 Pereverzev A, Mikhna M, Vajna R, Gissel C, Henry M, Weiergräber M, Hescheler J, Smyth N, Schneider T: Disturbances in glucose-tolerance, insulin-release and stress-induced hyperglycemia upon disruption of the Cav2.3 (a1E) subunit of voltage-gated Ca²⁺ channels. *Mol Endocrinol* 2002;16:884-895.
- 34 Jing X, Li DQ, Olofsson CS, Salehi A, Surve VV, Caballero J, Ivarsson R, Lundquist I, Pereverzev A, Schneider T, Rorsman P, Renstrom E: Ca(V)_{2.3} calcium channels control second-phase insulin release. *J Clin Invest* 2005;115:146-154.
- 35 Zhang Q, Bengtsson M, Partridge C, Salehi A, Braun M, Cox R, Eliasson L, Johnson PR, Renström E, Schneider T, Berggren PO, Gopel S, Ashcroft FM, Rorsman P: R-type calcium-channel-evoked CICR regulates glucose-induced somatostatin secretion. *Nat Cell Biol* 2007;9:453-460.
- 36 Helbig KL, Lauerer RJ, Bahr JC, Souza IA, Myers CT, Uysal B, Schwarz N, Gandini MA, Huang S, Keren B, Mignot C, Afenjar A, Billette de Villemeur T, Heron D, Nava C, Valence S, Buratti J, Fagerberg CR, Soerensen KP, Kibaek M, et al.: De Novo Pathogenic Variants in CACNA1E Cause Developmental and Epileptic Encephalopathy with Contractures, Macrocephaly, and Dyskinesias. *Am J Hum Genet* 2018;103:666-678.
- 37 Kuzmiski JB, Barr W, Zamponi GW, MacVicar BA: Topiramate inhibits the initiation of plateau potentials in CA1 neurons by depressing R-type calcium channels. *Epilepsia* 2005;46:481-489.
- 38 Oakley F, Horn NM, Thomas AL: Histidine-stimulated divalent metal uptake in human erythrocytes and in the erythroleukaemic cell line HEL.92.1.7. *J Physiol* 2004;561:525-534.
- 39 El Khoury Y, Hellwig P: Infrared spectroscopic characterization of copper-polyhistidine from 1,800 to 50 cm⁻¹: model systems for copper coordination. *J Biol Inorg Chem* 2009;14:23-34.
- 40 Remko M, Fitz D, Rode BM: Effect of metal ions (Li⁺, Na⁺, K⁺, Mg²⁺, Ca²⁺, Ni²⁺, Cu²⁺ and Zn²⁺) and water coordination on the structure and properties of L-histidine and zwitterionic L-histidine. *Amino Acids* 2010;39:1309-1319.
- 41 Marger L, Schubert CR, Bertrand D: Zinc: an underappreciated modulatory factor of brain function. *Biochem Pharmacol* 2014;91:426-435.
- 42 Assaf SY, Chung SH: Release of endogenous Zn²⁺ from brain tissue during activity. *Nature* 1984;308:734-736.
- 43 Sloviter RS, Zappone CA, Harvey BD, Frotscher M: Kainic acid-induced recurrent mossy fiber innervation of dentate gyrus inhibitory interneurons: possible anatomical substrate of granule cell hyper-inhibition in chronically epileptic rats. *J Comp Neurol* 2006;494:944-960.
- 44 Siapich SA, Banat M, Albanna W, Hescheler J, Lücke M, Schneider T: Antagonists of ionotropic gamma-aminobutyric acid receptors impair the NiCl₂-mediated stimulation of the electroretinogram b-wave amplitude from the isolated superfused vertebrate retina. *Acta Ophthalmol* 2009;87:854-865
- 45 Siapich SA, Wrubel H, Albanna W, Alnawaiseh M, Hescheler J, Weiergräber M, Lücke M, Schneider T: Effect of ZnCl₂ and chelation of zinc ions by N,N-diethylthiocarbamate (DEDTC) on the ERG b-wave amplitude from the isolated and superfused vertebrate retina. *Curr Eye Res* 2010;35:322-334.
- 46 Kang HW, Vitko I, Lee SS, Perez-Reyes E, Lee JH: Structural determinants of the high affinity extracellular zinc binding site on Cav3.2 T-type calcium channels. *J Biol Chem* 2010;285:3271-3281.
- 47 Lisman JE, Idiart MAP: Storage of 7 ± 2 short-term memories in oscillatory subcycles. *Science* 1995;267:1512-1515.
- 48 Fell J, Klaver P, Lehnertz K, Grunwald T, Schaller C, Elger CE, Fernandez G: Human memory formation is accompanied by rhinal-hippocampal coupling and decoupling. *Nat Neurosci* 2001;4:1259-1264.
- 49 Bartos M, Vida I, Jonas P: Synaptic mechanisms of synchronized gamma oscillations in inhibitory interneuron networks. *Nat Rev Neurosci* 2007;8:45-56.
- 50 Montgomery SM, Buzsaki G: Gamma oscillations dynamically couple hippocampal CA3 and CA1 regions during memory task performance. *Proc Natl Acad Sci U S A* 2007;104:14495-14500.
- 51 Jutras MJ, Fries P, Buffalo EA: Gamma-band synchronization in the macaque hippocampus and memory formation. *J Neurosci* 2009;29:12521-12531

- 52 Proddatur A, Yu J, Elgammal FS, Santhakumar V: Seizure-induced alterations in fast-spiking basket cell GABA currents modulate frequency and coherence of gamma oscillation in network simulations. *Chaos* 2013;23:046109.
- 53 Jiang X, Lachance M, Rossignol E: Involvement of cortical fast-spiking parvalbumin-positive basket cells in epilepsy. *Prog Brain Res* 2016;226:81-126
- 54 Krook-Magnuson E, Armstrong C, Oijala M, Soltesz I: On-demand optogenetic control of spontaneous seizures in temporal lobe epilepsy. *Nat Commun* 2013;4:1376.
- 55 Joksovic PM, Weiergraber M, Lee W, Struck H, Schneider T, Todorovic SM: Isoflurane-sensitive presynaptic R-type calcium channels contribute to inhibitory synaptic transmission in the rat thalamus. *J Neurosci* 2009;29:1434-1445.
- 56 Alnawaiseh M, Albanna W, Chen CC, Campbell KP, Hescheler J, Lüke M, Schneider T: Two separate Ni^{2+} sensitive voltage-gated Ca^{2+} channels modulate transretinal signalling in the isolated murine retina. *Acta Ophthalmologica* 2011;89:e579-e590.
- 57 Engel J Jr, da Silva FL: High-frequency oscillations - where we are and where we need to go. *Prog Neurobiol* 2012;98:316-318.
- 58 Sochivko D, Pereverzev A, Smyth N, Gissel C, Schneider T, Beck H: The $\alpha 1E$ calcium channel subunit underlies R-type calcium current in hippocampal and cortical pyramidal neurons. *J Physiol* 2002;542:699-710.